의학박사 학위논문

새로운 세포외 소포체 추출 시스템을 이용한 세포외 소포체 순환 RNA 분석과 대장암의 진단

Diagnosing colorectal cancer with extracellular vesicle derived circulatory RNA analysis using a novel extracellular vesicle isolation system

울 산 대 학 교 대 학 원

의 학 과

김 영 일

Diagnosing colorectal cancer with extracellular vesicle derived circulatory RNA analysis using a novel extracellular vesicle isolation system

지도 교수 임 석 병

이 논문을 의학박사 학위논문으로 제출함

2024년 8월

울 산 대 학 교 대 학 원

의 학 과

김 영 일

김영일의 의학박사 학위논문을 인준함

심사위원장 박 인 자 (인)

심사위원 임 석 병 (인)

심사위원 신 용 (인)

심사위원 이 종 률 (인)

심사위원 양 동 훈 (인)

울 산 대 학 교 대 학 원

2024년 8월

Abstract

Purpose

Early detection for colorectal cancer (CRC) is challenging and crucial for effective intervention, as the 5-year survival rate declines sharply in advanced stages. Recently, liquid biopsy including small extracellular vesicles (sEVs) have gained significance in CRC diagnosis. The aim of this study was to apply a novel sEV isolation system to analyze circulatory RNA expression in CRC patients compared to healthy population.

Methods

Blood plasma samples of 80 colorectal cancer patients and 20 healthy controls were obtained from the Biological Resource Center of Asan Medical Center in Seoul, Korea. The enrolled subjects included individuals with histologically confirmed stage 0-1 (n = 20), stage 2 (n = 20), stage 3 (n = 20), and stage 4 colorectal cancer (n = 20) with healthy controls (n = 20). Integrated tool for EV isolation, EV-derived protein and EV-derived nucleic acid (NA) extraction with EV enrichment (SF-ZAHVIS) was used to isolate sEVs from plasma samples. sEV derived microRNAs (miRNAs) and circular RNAs (circRNAs) were compared between healthy control and according to each cancer stage. The efficacy of the sEV isolation system was assessed through a comparison with conventional sEV isolation techniques (ultracentrifugation [UC] and total exosome isolation [TEI] methods).

Results

The SF-ZAHVIS demonstrated an effective approach for sEV isolation, yielding purity and concentration comparable to the established UC and TEI techniques. The SF-ZAHVIS system successfully extracted EV derived non-coding RNAs and detected potential CRC miRNA markers (miR-23a-3p, miR-92a-3p, miR-125a-3p, miR-150-5p). The relative expression level of miR-23a-3p, miR-92a-3p, and miR-125a-3p was significantly higher in the CRC samples compared to healthy control (P = 0.0014, 0.0002, and 0.0274, respectively). Expression level of miR-150-5p was significantly lower in the CRC group compared to healthy control ($P < 0.0001$).

Conclusion

The SF-ZAHVIS system is capable of isolating sEVs efficiently. By using this novel system, miRNAs could be assessed from blood plasma to detect CRC.

Contents

List of Tables

List of Figures

1. Introduction

Colorectal cancer (CRC) stands as third most prevalent malignant tumors globally. It poses a significant risk of metastasis and recurrence, ranking second as a cause of cancer-related deaths.[1] Diagnosing CRC at early stages offers crucial treatment opportunities, significantly reducing CRC-associated mortality rates. It is well-documented that the 5-year relative survival rate for CRC patients dramatically declines from approximately 90% in stages 1 and 2 to less than 20% in stage 4.[2] Colonoscopy serves as the gold standard for CRC diagnosis, providing the advantage of direct visualization of the entire colon and facilitating the immediate detection and removal of suspicious growths or precancerous polyps. Recent studies have shown the benefits of colonoscopy for preventing CRC and lower pathologic stages of CRC when screened by colonoscopy.[3,4] Despite its benefits, colonoscopy comes with certain limitations, including invasiveness and challenges related to cost and accessibility. It is reported that adherence to repeated colonoscopy screening is around 54 percent in people with high-risk adenomas at guideline-recommended interval.[5] Also, people with positive stool-based testing who need sequential colonoscopy received the required colonoscopy in only 50 to 87 percent.[6] Other diagnostic modalities such as computed tomography (CT), magnetic resonance imaging, and tissue biopsies are time-consuming and costly. Moreover, they are not suitable for frequent monitoring of patients.

Therefore, constant need for a more accessible, economic, and effective method of diagnosing colorectal cancer has been raised. One of the ideal specimen for cancer diagnosis is the peripheral blood as it can be readily extracted in a repeated manner.[7] Various liquid biopsies have been studied not only for colorectal cancer but also for other malignancies such as gastric, esophageal, pancreatic, and breast cancers for less invasive screening.[8,9] Blood circulating biomarkers can be analyzed in real-time with minimal invasiveness. Successful results regarding liquid biopsy include variations in the levels of circulating tumor DNA (ctDNA), enabling earlier detection of CRC of having approximately 10 months lead time compared to CT scans and serum carcinoembryonic antigen (CEA).[10] Also, the significance of small extracellular vesicles (sEVs, < 200 nm) in CRC diagnosis has garnered substantial attention.[11] EVs, present in various body fluids including plasma, serum, saliva, and urine, play crucial roles in biological processes by serving as intercellular messengers for exchanging biological substances between cells. Exosomes are small EVs (30-150nm) and were relatively considered less important, classified as “cellular dust” or even mere bags of cell’s garbage.[12] Since the mid 1990’s, the role of exosomes were found to be related to intracellular communication, antigen presentation and shuttling of biologic agents.[13] Exomes include proteins, nucleic acids (NAs), lipids, and metabolites which reflect

the genetic, epigenetic, and conditional composition of the parent cells. For that reason, tumor-derived exosomes originating from cancer cells have emerged as promising biomarkers for early cancer detection, potentially providing insights into the presence and progression of cancer.[14]

Among the cargo of exosomes, non-coding RNA (ncRNA)s such as exosome-derived circRNAs and miRNAs have attracted significant interest due to their roles in diverse cellular functions and their implications in several pathological processes. CircRNAs, typically larger than 200 nucleotides (nt), are ncRNAs that form closed-loop structures without 5′ and 3′ ends, and they are closely associated with the initiation and progression of cancers. They exhibit stability in blood and play critical roles in intercellular communication.[15] Similarly, miRNAs are small ncRNAs that have roles in CRC initiation, progression, and metastases by regulating translation and stability of specific mRNAs. miRNAs have been found to be extremely stable compared to RNA molecules in plasma, resistant to nuclease activity.[14] These ncRNAs are reported to be abundant in small EVs, enhancing the already stable feature and hence being optimal biomarkers using EV extraction.

The isolation of EVs and exosomes is paramount for obtaining reliable information on the sensitivity and accuracy of exosome-derived biomarkers.[16] Consequently, there has been a recent emphasis on the development of rapid and convenient techniques to isolate high-concentration and high-purity exosomes from limited samples. Ultracentrifugation (UC) and total exosome isolation (TEI) method are currently the more commonly used techniques for exosome isolation. However, it requires expensive ultracentrifuges and involves a complicated, labor-intensive, and time-consuming process. Furthermore, the physical damage caused by high-speed centrifugation can result in the loss of EV-derived biomarkers, thereby reducing detection sensitivity.[17] Therefore, the urgent need for the development of a novel method that can accurately, conveniently, and economically isolate high-concentration and high-purity exosomes is clear.

In this study, we have developed a syringe filter-based simple and fast system for sEV isolation using zeolite-amine (zeolite-NH_2) and hydrazides, termed as the SF-ZAHVIS system. We aim to extract sEVs from blood plasma and compare miRNA and circRNA expression of CRC patients to healthy population to diagnose CRC.

2. Materials and Methods

2.1 Collection of Clinical Samples

For the clinical validation of the SF-ZAHVIS system, the present study was approved by the Institutional Review Board of Asan Medical Center (IRB no. 2023-0484) and all participants provided informed consent prior to their inclusion. A total of 100 blood plasma samples were obtained from the Biological Resource Center (BRC) of Asan Medical Center in Seoul, Korea. Blood from the patient planned for surgery was collected in citrate tubes 1 day prior to operation, typically in two tubes (5cc each). The collected blood was centrifuged at 4℃, 3000rpm (1,900g) for 10 minutes. (Equipment used: Hanil Science Combi-514R). 1.5ml of the upper plasma layer was taken and transferred to an Eppendorf (EP) tube, then centrifuged again at 4℃, 13,100rpm (16,000g) for 10 minutes. (Equipment used: Eppendorf centrifuge-5415R). Approximately 1ml of the upper layer of centrifuged plasma was transferred to a cryotube for freezing. Blood plasma samples of healthy participants visiting the Health Screening & Promotion Center was obtained from BRC of Asan Medical Center.

All samples were stored in a liquid nitrogen tank (LN_2 tank) at -196℃ for preservation. The enrolled subjects included individuals with histologically or cytologically confirmed stage 0-1 CRC (n = 20), stage 2 CRC (n = 20), stage 3 CRC (n = 20), stage 4 CRC (n = 20), and healthy controls (n = 20). These samples were properly classified and utilized for subsequent analysis.

2.2 Nucleic acid marker selection

Initially, we selected eleven miRNAs known to be associated with the diagnosis and prognosis of CRC (miR-19, miR-21, miR-23, miR-92, miR-99, miR-125, miR-141, miR-150, miR-182, miR-223, and miR-1246) and the commonly used miRNA housekeeping gene U6 from literature search. Furthermore, we selected three CRC-related circRNAs markers (CircLPAR1, CircLONP2, and CircPNN) and synthesized primers for the quantitative polymerase chain reaction (qPCR) of circRNA and the commonly used GAPDH as circRNA housekeeping gene using the CircInteractome database and the NCBI primer design tool.[15,18-32]

2.3 Cell line culture

The human colorectal carcinoma cell line HCT116 (ATCC #CCL-247) and the normal human colon cell line CCD-18Co (KCLB #21459) were obtained from the American Type Culture Collection and the Korean Cell Line Bank, respectively. Both cell lines were cultured under standard conditions at 37°C and 5% CO_2. The Dulbecco's modified Eagle medium (DMEM) medium was supplemented with

10% exosome-depleted fetal bovine serum (FBS) and a cocktail of antibiotic-antimycotic. For the isolation of EVs from both HCT-116 and CCD-18Co cells, the cells were grown until they reached around 80% confluence. The cell cultures were then centrifuged at 400g for 30 minutes at 4°C to obtain the cell-free supernatant. After filtration using a Polyvinylidene Fluoride (PVDF) 0.22 μm syringe filter, these supernatants were either immediately utilized for EV isolation via the SF-ZAHVIS system, UC, and TEI methods, or stored at -20°C for up to 4 weeks. 100X antibiotic–antimycotic (#15240062), exosome-depleted FBS (#A2720803), DMEM (#41965039) and RPMI 1640 Medium (#A1049101) were sourced from Gibco.

2.4 Workflow of the SF-ZAHVIS system

The zeolite-NH_2 utilized in the SF-ZAHVIS system was synthesized as following. A total of 3g of zeolite was washed twice for 10 minutes at 550 rpm using dextrose water (DW) and 95% ethanol. To ensure the uniformity of the zeolite size, larger particles that had precipitated within a minute were removed during the first washing step. After each wash, the washed zeolite was briefly centrifuged at 1,000 rpm for 10 seconds, and the supernatant was discarded to eliminate smaller-sized particles. The zeolite was then subjected to amine group functionalization, achieved by incubating it in a 2% 3-Aminopropyl(diethoxy) methyl silane (APDMS) solution in 95% ethanol for 4 hours at 450 rpm. The synthesized zeolite-NH_2 was washed three times for 5 minutes at 550 rpm using DW and 95% ethanol. Following these steps, the zeolite-NH_2 was left to dry completely in a vacuum chamber for over 24 hours. The dried zeolite-NH_2 was stored at room temperature until further use.

The SF-ZAHVIS system is an integrated tool for sEV isolation, sEV-derived protein and sEV-derived NA extraction, with sEV enrichment. Initially, zeolite-NH_2 and malonic acid dihydrazide (MDH) were mixed per 1 mL of the prepared biological sample and incubated for 10 minutes. This mixture was then transferred into a suitable volume Kovax syringe and connected to a PVDF 0.45 μm syringe filter. By gently pressing the syringe by hand, all unreacted waste was removed. Then, the concentrated EVs bound to the zeolite-NH_2 on the filter surface were washed with phosphate buffered saline (PBS). The isolation of sEVs was achieved by injecting 300 μL of high pH elution buffer, including 10 mM sodium bicarbonate at pH 10.4, via a BD 1 mL syringe and incubating for 1 minute. Subsequently, EVs detached from the zeolite-NH_2 surface were separated by injecting air. For EV-derived protein extraction, 300 μL of Radio-immunoprecipitation assay (RIPA) lysis buffer was injected using a BD 1 mL syringe, followed by 20 minutes incubation at 4°C. Proteins from EVs within the RIPA lysis buffer were then extracted by air injection. For the extraction of NAs from EVs, 300 μL of NP-40 lysis buffer containing

7.5 mg of MDH was injected using a BD 1 mL syringe and incubated at room temperature for 20 minutes. The EV-derived proteins were removed via air injection, followed by a wash with 3 mL of PBS and removal of residual PBS within the filter. Finally, the EV-derived NAs were eluted by injecting 300 μL of high pH elution buffer via a BD 1 mL syringe and incubating for 1 minute. The NAs detached from the zeolite-NH_2 surface were then separated by injecting air (Figure 1). Zeolite (#96096) and 3-APDMS (#371890) were acquired from Sigma-Aldrich. Malonic acid dihydrazide (#M3206) was sourced from Tokyo Chemical Industry. Kovax 1–30 mL and BD 1 mL syringe (#309628) were obtained from Korea Vaccine and Becton, Dickinson and Company, respectively. Polytetrafluoroethylene (PTFE) 3 μm syringe filter (#18140), PTFE 1 μm syringe filter (#16278), PVDF 3 μm syringe filter (#18215), PVDF 1 μm syringe filter (#18214) were obtained from Tisch Scientific. PVDF 0.22 μm syringe filter (#FJ25ASCCA002DL01) and PVDF 0.45 μm syringe filter (#FJ25ASCCA004FL01) were supplied by GVS Filter Technology. RIPA lysis and extraction buffer (#89901) from Thermo Scientific and NP-40 lysis buffer (#J60766) from Alfa Aesar were used for EV lysis.

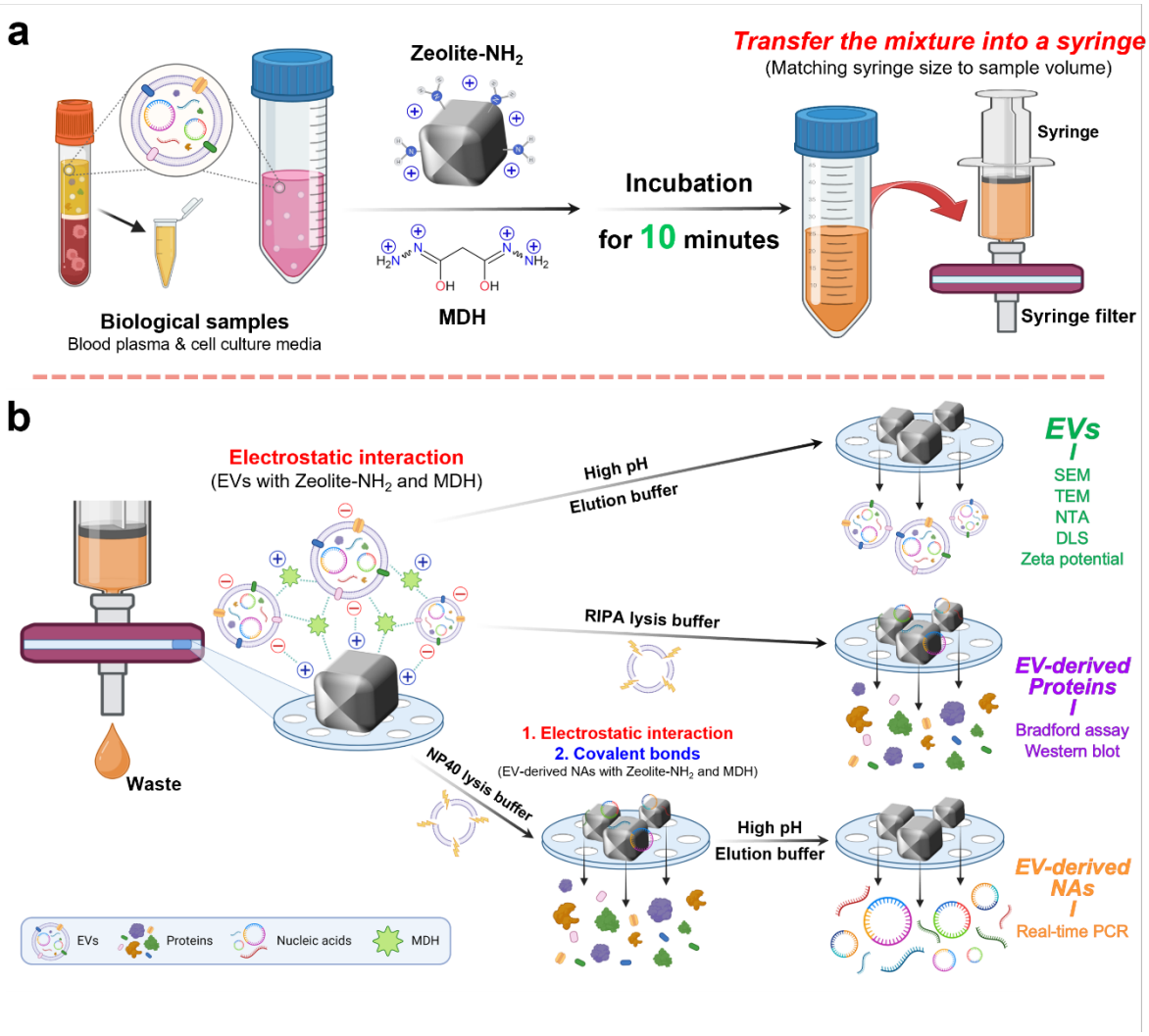

Figure 1. Schematic illustration of application of the SF-ZAHVIS system. (a) Preparation of materials such as zeolite-NH_2, MDH, and syringe filter and workflow for enrichment of EVs using biological samples (b) Workflow and mechanism of EV isolation, EV-derived proteins and nucleic acids extraction.

2.5 EV isolation and characterization

In order to validate the SF-ZAHVIS system, we employed traditional methods of EV isolation, including UC and TEI methods. For UC, 10 mL of cell culture medium was subjected to centrifugation at 110,000 g for 70 minutes at 4°C, after which the supernatant was discarded, leaving the EV pellet. The TEI method involved mixing 10 mL of cell culture medium with 5 mL of TEI reagent. The mixture was then incubated overnight at 4°C, followed by centrifugation at 10,000 g for 60 minutes at 4°C and the supernatant was discarded. The EV pellet in both methods was reconstituted in either 300 μL of PBS for EV collection or in 300 μL of RIPA lysis buffer for EV-derived protein extraction. The isolated EVs were characterized by their morphology, count, diameter, and surface properties via scanning electron microscopy (SEM), transmission electron microscopy (TEM), nanoparticle tracking analysis (NTA), dynamic light scattering (DLS), and zeta potential analyses. Furthermore, the Bradford assay and western blot analysis were performed to determine the protein concentration and identify marker proteins of extracted EV-derived proteins.

The morphology of the sEVs isolated using the SF-ZAHVIS system, UC, and TEI methods was assessed using TEM and SEM. For TEM imaging, we diluted the EVs 1:10 in PBS and incubated them on a Formvar/carbon-coated copper grid at 37°C for 30 minutes. For CD9 labeling, the grid was initially blocked with 5% BSA for 20 minutes, and then incubated with a 10 nm gold tagged CD9 antibody, diluted according to the manufacturer's instructions, at 4°C overnight. For both blank and CD9 labeling images, the grids were treated with 2.5% glutaraldehyde and 3% citrate solution for 5 minutes each, washed with DW, and placed on parafilm. These grids were left to dry overnight in a fume hood. The TEM images were visualized with a JEM-ARM200F device (JEOL, Japan). For SEM imaging, we diluted the EVs at a ratio of 1:10 in PBS and placed drops on a silicon wafer, which we left at 37°C for 30 minutes. We then fixed the wafer for 10 minutes using 2.5% glutaraldehyde. We soaked the wafers in different percentages of ethanol (30%, 50%, 70%, 80%, 90%, and 100%) for 15 minutes each time. After dried in a fume hood, we covered the wafers with a thin layer of platinum (Pt) and captured images using a JSM-7610F-Plus device (JEOL). Glutaraldehyde (#340855) was acquired from Sigma-Aldrich. Invitrogen supplied the Total Exosome Isolation Reagent (#4478359).

To determine the quantity, diameter distribution, and surface properties of the EVs, we performed NTA, DLS, and zeta potential analysis following standard protocols. We resuspended the separated EVs in PBS at ratios of 1:50 or 1:100 and injected them into cuvettes. For the NTA, we used the NS300 instrument and NanoSight software (Malvern Panalytical Ltd. United Kingdom) to measure the concentration and intensity distribution of EVs. The number distribution of EVs was measured using

DLS with the ELS-Z1000 instrument (Otsuka Electronics, Japan) and Photal software (Otsuka Electronics). The surface charge of EVs was measured with a NANO ZS 90 instrument (Malvern Panalytical).

2.6 Western blot analysis, Real-time PCR, and relative quantification (RQ)

EV-derived proteins extracted from the SF-ZAHVIS system, UC, and TEI methods were analyzed. Protein concentration was determined using the Bradford assay, with a series of BSA dilutions as the standard. Equal protein amounts (20 μg) were separated on 10% SDS-PAGE and transferred to a PVDF microporous membrane. The membrane was blocked for 1 hour in PBS-Tween 20 containing 5% skim milk. Primary antibodies (CD9, CD63, CD81, ARF6, GRP78, GM130, and Calnexin) were diluted following the manufacturer's instructions and incubated overnight at 4°C. The membranes were then put in a solution of HRP-tagged secondary antibodies diluted again according to the instructions from the manufacturer for 1 hour. Marker proteins were detected using a 1:1 mixture of peroxidase and chemiluminescent substrate, and images were captured with a ChemiDoc MP Imaging System (Bio-Rad) and Image Lab software (Bio-Rad). The antibodies included Rabbit Anti-CD9 antibody (#ab236630), Rabbit Anti-CD63 antibody (#ab134045), Mouse Anti-CD81 antibody (#ab79559), Rabbit Anti-ARF6 antibody (#ab131261), Rabbit Anti-GRP78 antibody (#ab108615), Rabbit Anti-GM130 antibody (#ab52649), Goat Anti-Rabbit IgG/HRP antibody (#ab205718), Goat Anti-Mouse IgG/HRP antibody (#ab6789), Donkey Anti-Rabbit IgG/Gold antibody (#ab39597) from Abcam Plc, and Rabbit Anti-Calnexin antibody (#2679S) from Cell Signaling Technology.

We employed the Mir-X miRNA qRT-PCR TB Green Kit for miRNA cDNA synthesis and qPCR analysis. The process involved mixing 4 μl of sEV-derived NAs from the SF-ZAHVIS sample with 5 μl of reaction buffer and 1 μl of reverse transcription enzyme, followed by an hour of incubation at 37 ˚C. After inactivating the enzyme at 85 ˚C for 5 minutes, we added 90 μl of RNase-free water to the reagent, and the 100 μl of synthesized cDNA was stored at -20 ˚C for future use. For the qPCR of miRNA, we combined the cDNA with miRNA-specific forward primer, mRQ 3′ reverse primer, and TB green premix. The amplification protocol consisted of an initial denaturation step at 95 ˚C for 10 s, followed by 40 cycles of 5 s at 95 ˚C and 20 s at 60 ˚C and a final melt curve stage. Mir-X miRNA qRT-PCR TB Green Kit (#638314) was obtained from Takara. The oligonucleotides used were purchased from BIONICS and Macrogen.

For circRNA in qPCR analysis, we used the SuperScript IV First-Strand Synthesis System with a 50 μM random hexamer for denaturing template RNA. After combining the 11 μl of sEV-derived circRNA

samples from the SF-ZAHVIS with reaction buffer and reverse transcription enzyme, we incubated the 20 µl of combined reaction mixture for 10 minutes at 23 ˚C, 10 minutes at 50 ˚C, and 10 minutes at 80 ˚C. We then added 30 µl of RNase-free water to the synthesized cDNA and stored it at -20 ˚C until use. For qPCR analysis of circRNA, we mixed 5 µl of synthesized cDNA and primer sets with Brilliant III SYBR Green QPCR Master Mix. The amplification protocol consisted of an initial denaturation step at 94 ˚C for 2 min, followed by 50 cycles of 15 s at 94 ˚C, 30 s at 55 ˚C, and 1 min at 68 ˚C. The amplification concluded with a final melt curve stage. Invitrogen supplied the SuperScript IV First-Strand Synthesis System (#18091050) and Brilliant III SYBR Green QPCR Master Mix (#600882) was supplied by Agilent Technologies.

To calculate the RQ of miRNA and circRNA candidates, U6 snRNA and GAPDH were utilized as internal control genes to normalize miRNA and circRNA expression levels, respectively. The gene expression quantification was carried out by following these steps: (1) The difference in threshold cycle (ΔCt) was computed by subtracting the Ct value of the reference gene from the Ct of the target gene. (2) The ΔCt value for CRC samples were then normalized to the average ΔCt of the healthy control group, resulting in ΔΔCt. (3) Finally, the RQ was calculated using the formula $2^{-\Delta\Delta Ct}$.

2.7 Statistical analysis

Statistical analyses were performed using IBM SPSS Statistics version 27.0 (IBM Corp., Armonk, NY, USA), GraphPad Prism software version 8.0.1 (GraphPad Software, La Jolla, CA, USA), and Python version 3.10.13. Python was specifically utilized to compute the Receiver Operating Characteristic (ROC) curve and the Area Under the Curve (AUC) with the Scikit-learn library. The ROC curve was visualized using the Matplotlib library, with figures generated via GraphPad Prism software. The Mann-Whitney U-test was employed to compare continuous variables after assessing the data distribution using the Kolmogorov-Smirnov test and Shapiro-Wilk test. All results are representatives of at least three independent experiments. For all statistical tests, *P*-values less than 0.05 were considered statistically significant.

3. Results

3.1 SF-ZAHVIS system compared to UC and TEI

The efficacy of the SF-ZAHVIS system was assessed through a comparison with commonly employed EV isolation techniques, specifically the UC and TEI methods. Initially, we verified the morphology of EVs isolated by each method through blank TEM and SEM images, which revealed spherical sEVs of approximately 100 nm in size in all cases (Figure 2a–c). Furthermore, we confirmed the presence of CD9, a specific marker protein from the tetraspanin family for sEVs, using 10 nm gold particles for immuno-labeling (Figure 2d–f). EV's particle size distribution, based on signal intensity and number, was determined through NTA (SF-ZAHVIS for 187.1 ± 27.5, UC for 202.4 ± 36.7, and TEI for 222.5 ± 65.3, nm) and DLS (SF-ZAHVIS for 172.2 ± 34.0, UC for 176.3 ± 26.2, and TEI for 114.2 ± 26.7, nm) analysis. Additionally, we noted that isolated EVs possessed zeta potentials between -10 and -25 mV (SF-ZAHVIS for -21.1 ± 2.57, UC for -15.53 ± 1.56, and TEI for -10.67 ± 0.91), indicating a negative charge (Figure 2g). The ratio of particle number to protein concentration in the isolated EVs is a crucial metric, indicating the concentration and purity of sEVs, with a higher ratio suggesting successful isolation due to the increased particle concentration. The SF-ZAHVIS system achieved sEV isolation with a high concentration and purity comparable to the UC ($5.45 \times 10^{10} \pm 2.68 \times 10^{9}$) and TEI ($5.27 \times 10^{10} \pm 3.19 \times 10^{9}$) methods, as indicated by a particle/protein concentration ratio of $5.26 \times 10^{10} \pm 1.16 \times 10^{9}$ (Figure 2h). Next, to determine the quantity and purity of the extraction of EV-derived proteins by the SF-ZAHVIS system and confirm the presence of sEV specific proteins, we conducted a western blot analysis for sEV-specific proteins (CD9, CD63, and CD81) as well as non-specific proteins (ARF6, GRP78, GM130, and Calnexin). As seen in Figure 2i, all three techniques demonstrated the presence of the representative sEV markers belonging to the tetraspanin family, namely CD9, CD63, and CD81. Furthermore, the presence of microvesicle marker ARF6, apoptotic body marker GRP78, Golgi marker GM130, and endoplasmic reticulum marker Calnexin was not observed, thus confirming the lack of contaminant proteins in the isolated sEVs (Figure 2j).

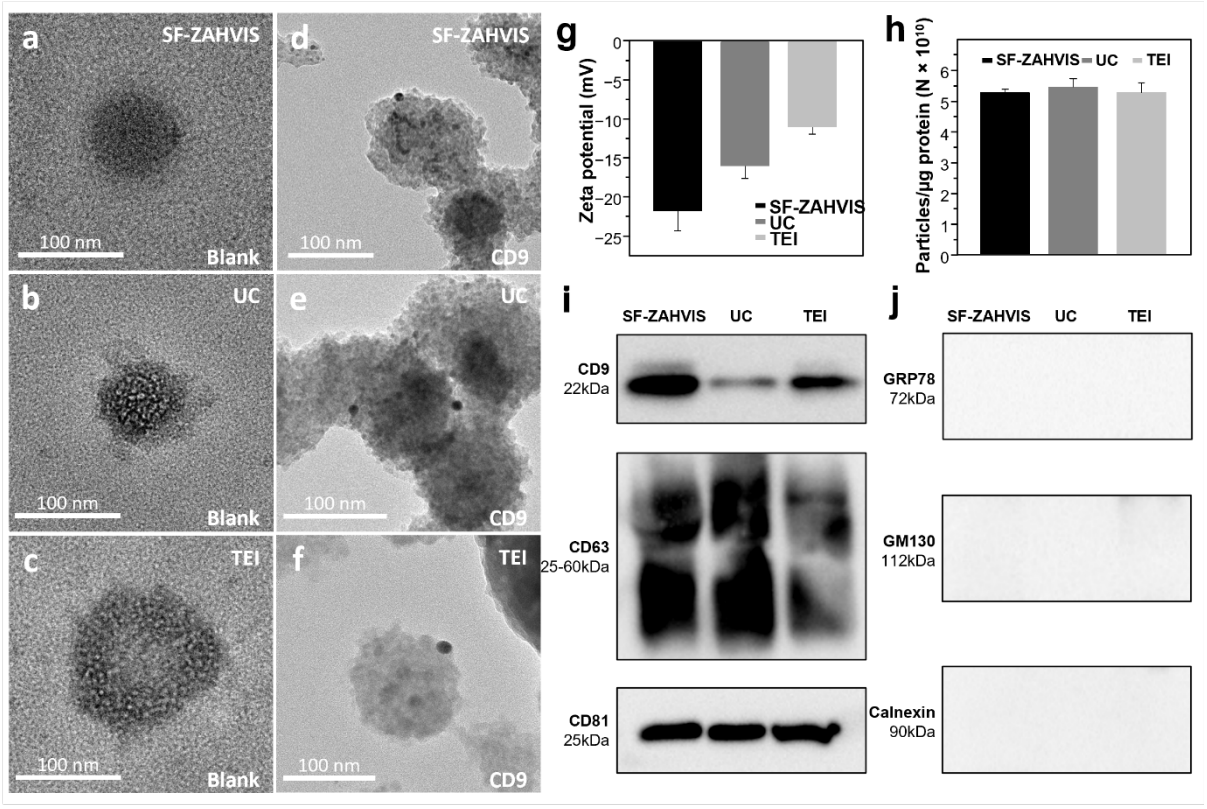

Figure 2. Comparison of the SF-ZAHVIS system with conventional methods. Representative TEM images of EVs obtained from (a) the SF-ZAHVIS system, (b) UC, and (c) TEI methods. Representative TEM images of CD9-labelled EVs acquired from (d) the SF-ZAHVIS system, (e) UC, and (f) TEI methods. (g) Zeta potential of isolated EVs. (h) Purity of EVs based on the ratio of EV particle concentration to protein concentration, determined using NTA and Bradford assay. (i) Western blot analysis for the detection of sEV-specific tetraspanin family proteins (CD9, CD63, and CD81), and (j) non-specific protein markers (ARF6 for microvesicles, GRP78 for apoptotic bodies, GM130 for Golgi apparatus, and Calnexin for Endoplasmic Reticulum). Error bars represent the standard deviation for a single experiment ($N \geq 3$).

3.2 Marker selection in cell cline culture

To assess the SF-ZAHVIS system in extracting EV-derived NAs and to detect CRC-related biomarkers, we analyzed non-coding RNAs from EVs extracted from the cell culture medium of the CRC cell line HCT116 using real-time PCR (qPCR). All primers utilized in the qPCR were provided in Table 1. We analyzed the pre-selected eleven miRNAs known to be associated with the diagnosis and prognosis of CRC (miR-19, miR-21, miR-23, miR-92, miR-99, miR-125, miR-141, miR-150, miR-182, miR-223, and miR-1246). SF-ZAHVIS system successfully extracted EV-derived ncRNAs and detected all potential CRC miRNA markers. Amongst the miRNA markers, miR-19a-3p, miR-21-5p, miR-23a-3p, miR-92a-3p, miR-125a-3p, miR-150-5p, and miR-1246 presented significantly different expression between the cancer cell line and normal colon cell line (*P* values of 0.0022, 0.0022, 0.0022, 0.0043, 0.0043, 0.0022, and 0.0022 respectively) (Figure 3).

Furthermore, we analyzed three CRC-related circRNAs markers (CircLPAR1, CircLONP2, and CircPNN) and synthesized primers for the qPCR of circRNA. Similar to EV-derived miRNAs, we confirmed that the SF-ZAHVIS system is capable of extracting EV-derived circRNAs, and all three biomarkers were detected. All three circRNAs (CircLPAR1, CircLONP2, and CircPNN) presented significant difference in expression between the cancer cell line and normal colon cell line (*P* values of 0.0022, 0.0022, and 0.0152 respectively) (Figure 4).

3.3 MicroRNA markers analysis in blood plasma of CRC patients and healthy population

Biomarkers with significantly different expression in the cell line cultures were analyzed in clinical samples. MicroR-23a-3p, miR-92-3p, and miR-125a-3p presented significantly higher expression in the CRC samples compared to the samples of healthy population (*P* values of 0.0014, 0.0002, and 0.0274 respectively). CRC samples showed significantly lower expression of miR-150-5p ($P < 0.0001$) compared to healthy samples (Figure 5a).

ROC curves estimating the performance of each biomarkers distinguishing CRC from healthy samples are depicted in figure 5b. The highest AUC was presented by miR-150-5p with 0.85. F1 score was highest in miR-23a-3p with 80.27% and miR-150-5p with 79.41% (Figure 5b). Other miRNAs and circRNAs showed no significant difference in expression between the CRC samples and healthy samples (Figure 6).

Among the markers which showed significantly distinctive expression, miR-23a-3p and miR-150-5p presented significant difference in all four stages of CRC compared to healthy control. MicroR-92a-3p did not present significant difference in stage 0-1 patients and miR-125a-3p did not show significant

difference in stage 3 and stage 0-1 (Table 2).

The miRNAs that presented significant expression difference in CRC samples were compared between each cancer stages. There was no inter-stage difference in any of the four markers (Table 3).

Table 1. Primer sets for detection of EV-derived RNAs (miRNAs and circRNAs) associated with CRC used in this study.

	Target	Location	Sequence (5'–3')	Length (bp)
Micro RNAs	*hsa-miR-19a-3p*	Forward	TGT GCA AAT CTA TGC AAA ACT GA	23
	hsa-miR-21-5p	Forward	TAG CTT ATC AGA CTG ATG TTG A	22
	hsa-miR-23a-3p	Forward	ATC ACA TTG CCA GGG ATT TCC	21
	hsa-miR-92a-3p	Forward	TAT TGC ACT TGT CCC GGC CTG T	22
	hsa-miR-99b-5p	Forward	CAC CCG TAG AAC CGA CCT TGC G	22
	hsa-miR-125a-3p	Forward	ACA GGT GAG GTT CTT GGG AGC C	22
	hsa-miR-141-3p	Forward	TAA CAC TGT CTG GTA AAG ATG G	22
	hsa-miR-150-5p	Forward	TCT CCC AAC CCT TGT ACC AGT G	22
	hsa-miR-182-5p	Forward	TTT GGC AAT GGT AGA ACT CAC ACT	24
	hsa-miR-223-3p	Forward	TGT CAG TTT GTC AAA TAC CCC A	22
	hsa-miR-1246	Forward	AAT GGA TTT TTG GAG CAG G	19
	Universal	Reverse	mRQ 3' Primer from TAKARA	.
	U6	Forward	CTC GCT TCG GCA GCA CA	17
		Reverse	AAC GCT TCA CGA ATT TGC GT	20
Circular RNAs	*circLPAR1*	Forward	GTA GTT CTG GGG CGT GTT CA	20
		Reverse	TAG GTG GAT GGG GAG CTT CA	20
	circLONP2	Forward	GTG AAG GTG GCA GAA GGA CA	20
		Reverse	TGG GTT GTT CAC TCC CAC AG	20
	circPNN	Forward	CCT GGA AGA ATG TGT CCA GCT A	22
		Reverse	GCT TTC TCT CTT CTT CTG CCT G	22
	GAPDH	Forward	TAT CGT GAT GCT AGT CCG ATG	21
		Reverse	TGC AGC TAG CTG CAT CGA TCG G	22

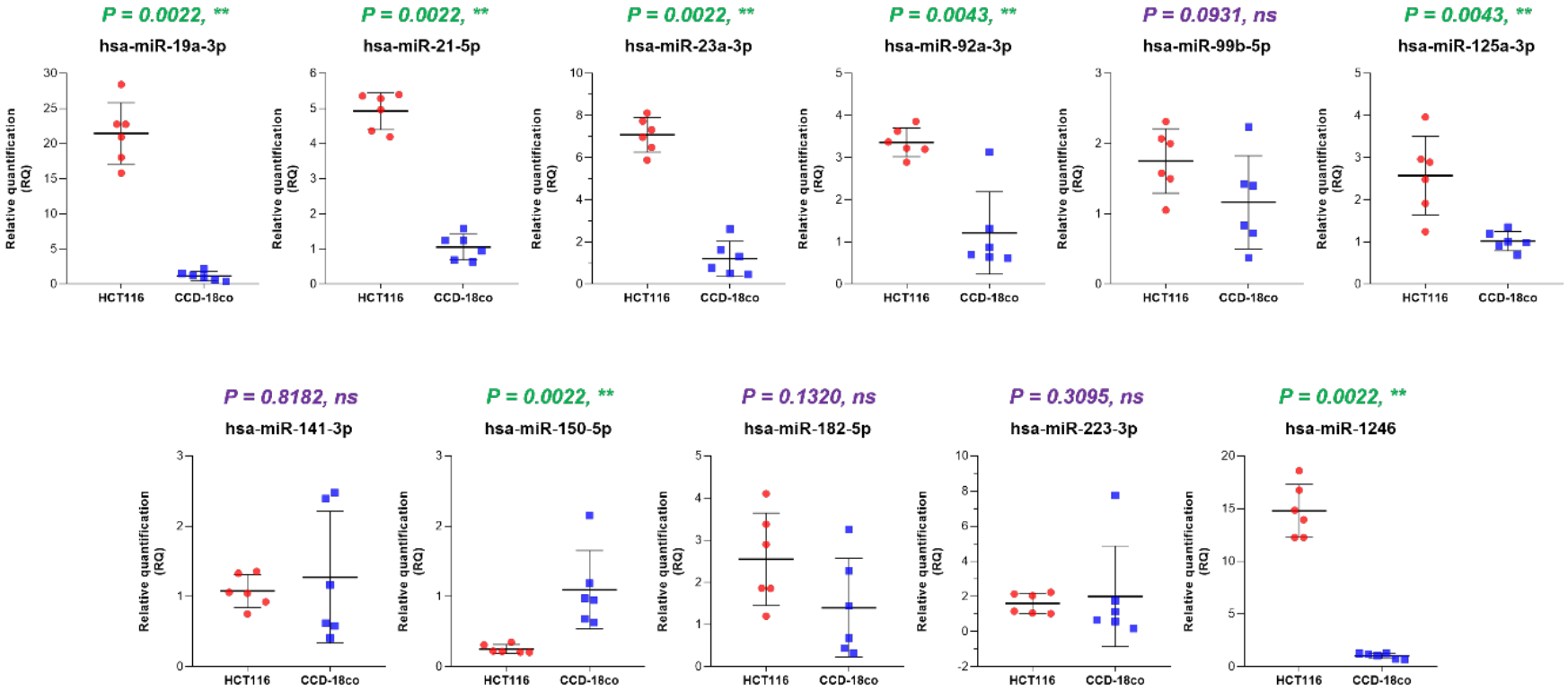

Figure 3. miRNA expression in colorectal cancer cell line compared to normal cell line.

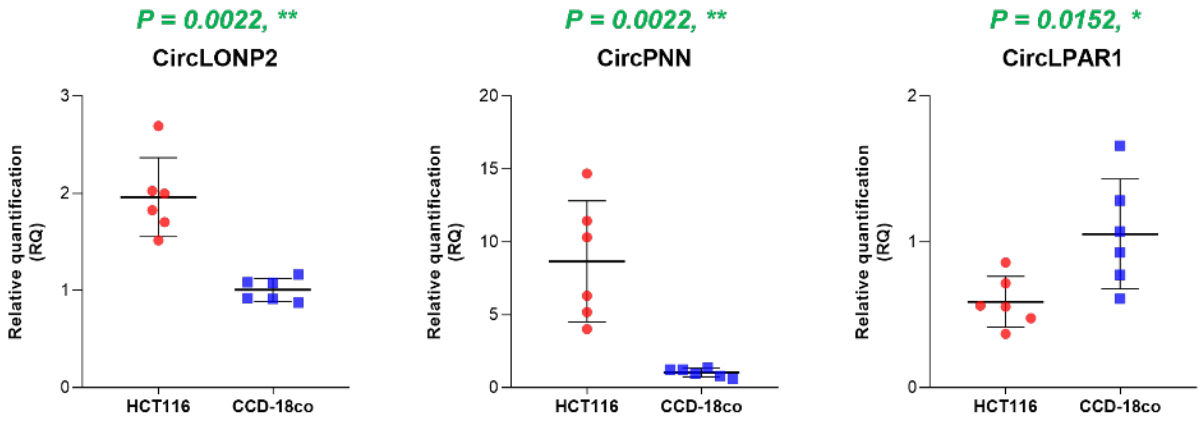

Figure 4. circRNA expression in colorectal cancer cell line compared to normal cell line.

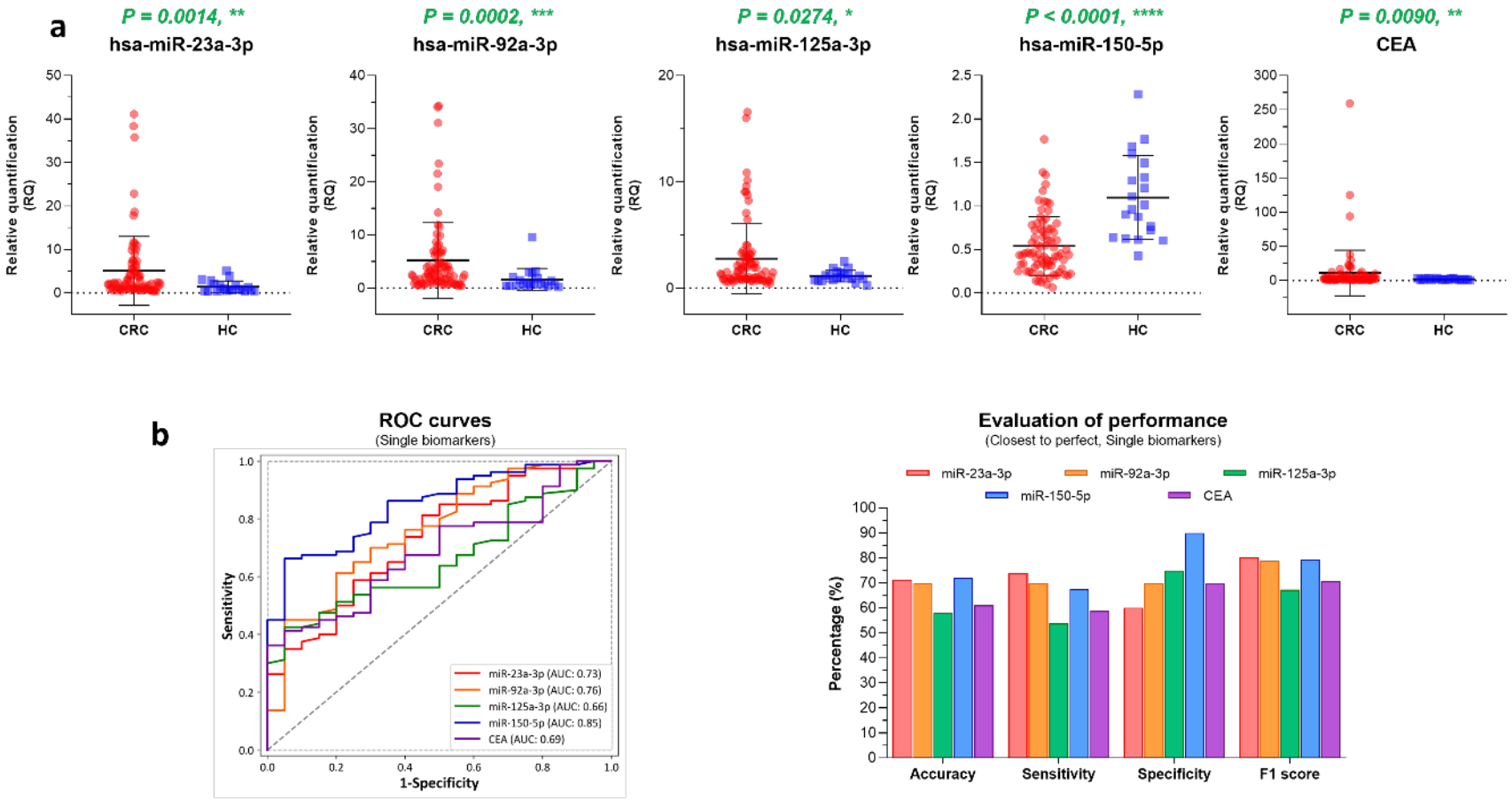

Figure 5. (a) Significant miRNA expressions in CRC plasma compared to plasma of healthy population. (b) ROC curves estimating the performance of percentages distinguishing CRC from healthy samples.

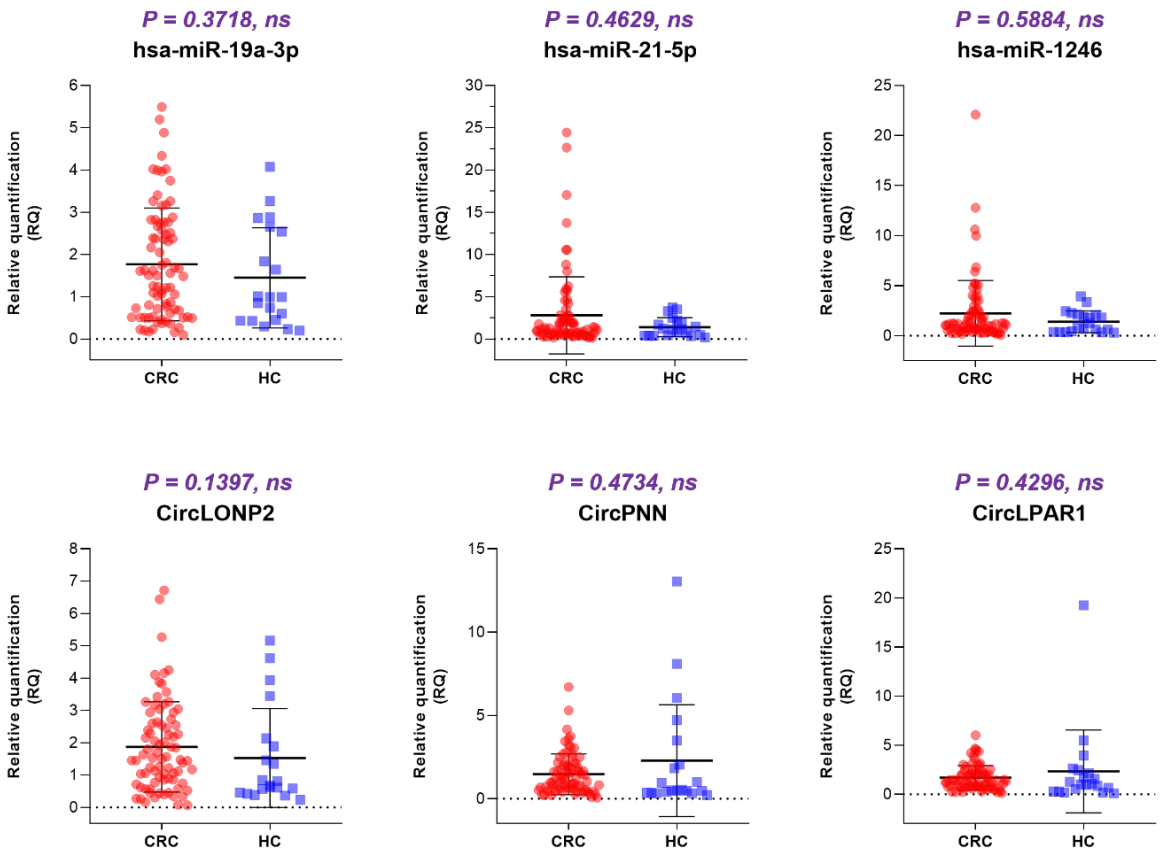

Figure 6. Unsignificant miRNA and circRNA expressions in CRC plasma compared to plasma of healthy population.

Table 2. miRNA expression compared between each CRC stages and healthy control (*P* values).

Marker	CRC vs HC	CRC stage 4 vs HC	CRC stage 3 vs HC	CRC stage 2 vs HC	CRC stage 0/1 vs HC
miR-23a-3p	0.0014	0.026	0.004	0.018	0.012
miR-92a-3p	0.0002	0.001	0.012	< 0.0001	0.052
miR-125a-3p	0.0274	0.003	0.414	0.023	0.369
miR-150-5p	< 0.0001	< 0.0001	0.012	< 0.0001	< 0.0001

Table 3. miRNA expression compared between each CRC stages (*P* values).

Marker	CRC stage 4 vs 3	CRC stage 4 vs 2	CRC stage 4 vs 0/1	CRC stage 3 vs 2	CRC stage 3 vs 0/1	CRC stage 2 vs 0/1
miR-23a-3p	0.9680	0.9680	0.6980	0.9467	0.6783	0.9254
miR-92a-3p	0.1826	0.8410	0.1493	0.1653	0.7584	0.0810
miR-125a-3p	0.0675	0.7994	0.1022	0.1826	0.9254	0.2012
miR-150-5p	0.2648	0.6395	0.6395	0.5291	0.0718	0.4135

4. Discussion

This study examined the efficacy of a new sEV isolation system designed for more simple and practical extraction of sEVs and following CRC biomarker analysis. The SF-ZAHVIS was able to extract sEVs efficiently, comparable to UC and TEI methods. NA markers analyzed from CRC patient plasma using this novel method showed significantly high expressions of miR-23a-2p, miR-92a-3p, miR-125a-3p, and low expression in miR-150-5p compared to healthy population. These results contribute to the growing interest in utilizing sEVs for cancer diagnosis.

The use of blood based liquid biopsies to early diagnose CRC and identify minimal residual disease (MRD) in CRC has been studied extensively to date. Various cancer derived components circulating in patient plasma such as circulating tumor cells (CTC), ctDNA, ncRNAs such as miRNA and circRNA, proteins, and EVs including exosomes are rising candidates for new diagnostic biomarkers. For instance, ctDNA has been reported to be accurate in detecting MRD of CRC after primary tumor resection and can predict recurrence.[8] With this result, further application of liquid biopsy was able to proficiently aid clinicians in actual decision making for the administration of chemotherapy.[33] However, screening and early diagnosis of CRC has proven to be difficult with the new liquid-based markers due to its low detection rate and lower sensitivity in early CRC compared to advanced CRC.[34,35] The median sensitivity of a multi-analyte blood test assessing levels of circulating proteins and mutations in cell-free DNA for stage I cancers were 43 percent compared to 73 and 78 percent in stage II and III respectively.[35] Another study showed 50 percent of stage I CRC patients with ctDNA alterations compared to 89, 90, and 93 percent in stage II, III, and IV CRC patients respectively.[34] Early CRC tend to have smaller tumor size and therefore excrete minimal quantities of DNA into patient bloodstream. In addition, identifying significant genetic alterations without the knowledge of genetic composition of the original primary tumor is challenging.

Other than ctDNA, miRNAs in blood samples have shown its role related to various human cancer.[21,36-38] miRNAs are small ncRNAs that regulate translation and stability of target mRNAs, and has been shown to be deeply involved in cancer biology; regulation of cellular development, differentiation, proliferation, apoptosis, and metabolism.[38,39] Although miRNAs were initially thought to be globally reduced in cancer, following studies show that miRNAs have both oncogenic and tumor suppressive functions and CRC in particular, more oncogenic.[40] Ng et al. performed a comparison study between 90 patients with CRC and 50 healthy control, assessing miRNA expression using RT-PCR-based miRNA profiling from plasma samples. miR-92 was significantly elevated in patients with CRC ($P < 0.0005$), showing the potential of miRNAs for CRC screening.[41] Upregulation of miR-92a in cancer is

reported by several other studies and has been shown to promote proliferation, invasion, and migration of CRC through the RECK-MMP signaling pathway as well as targeting KLF4 and downstream p21. This is associated with poor prognosis in CRC.[20,42] The results from the present study showing significant upregulation of mi-92a in CRC is in accordance with previous results. Also in CRC, miR-23a is known to promote the transition of indolent to invasive CRC, functionally promoting migration and invasion of cancer cells.[19,43] Additionally, down regulated serum exosomal miR-150-5p in CRC patients compared to healthy population has been previously reported using exosome isolation by UC.[18] These results correlate with the findings from the present study, providing further evidence of diagnostic values of such biomarkers in CRC.

Another ncRNA recently taking attention in cancer management is the circRNAs. CircRNAs are single-stranded RNAs generated from back-splicing of pre-messenger RNAs. Structured as a covalently closed continuous loop, circRNAs are more stable and resistant to exonucleases compared to linear RNAs.[44] In the past they were considered as products of molecular accidents during splicing or other insignificant pathogens.[45,46] However, recent researches identified circRNAs as a type of endogenic ncRNA that has tissue specific expression patterns, and is also related to the development of various cancers.[47,48] CircRNAs interact with miRNAs and act as sponges or decoys, limiting miRNAs actions for control of gene expression. This is relevant to cancer cell proliferation, migration, and angiogenesis. Specifically, circPACRGL has been identified to promote cell proliferation, migration, invasion, and neutrophil differentiation.[15] CircLONP2 has been reported to be upregulated in CRC patients with poor prognosis and directly interacts with miR-17 which enhanced the cancer cell aggressiveness.[31] In top of the exceptionally stable characteristic, circRNAs are especially abundant in sEVs, and exosomal circLPAR1 was previously reported to be markedly down regulated in CRC patients[30], while exosomal circPNN was significantly upregulated compared to healthy control group.[49] Unfortunately, the results from the present study revealed no significant difference between CRC and healthy control clinical samples. On the other hand, analyses of circRNAs in cell line showed significant upregulation of circPNN, circLONP2 and down regulation of circLPAR1, which is in accordance with previously reported studies.

To date, many studies have reported various results on different ncRNAs in CRC. However, the results are not always unified, e.g., the upregulation of miR125a-3p in the present study is contradicted by other studies showing inhibition of CRC proliferation by miR-125.[22] It has been shown that the different methods for isolating sEVs from various biological fluids result in significantly different yield and purity of the physical characters of sEVs and also its compositions including miRNAs and proteins.[50]

Also, the type of biological fluid used for analysis is known to differ in ncRNAs expression profile.[51] Therefore, the aim to apply optimal method of exosome isolation to the apposite biological fluid is still unresolved. Nevertheless, extraction of circulating EVs and analyzing biomarkers within the EVs has advantages compared to freely circulating biomarkers. The biomarkers including NAs are protected my lipid bilayer of the sEVs from degradation by proteases and nucleases.[52] Therefore, biomarker expressions assessed from EV-derived markers can reflect a more preserved status of the tumor that excrete the specific sEVs.[53] This is shown in a study by Dohmen et al. where the authors compared exosomal miRNAs and free circulating miRNAs in CRC. Significantly different expression was noted between the exosomal miRNAs of CRC and healthy controls but there was no significant difference noted in the free circulatory miRNAs.[54] Yet, studies directly comparing circulating biomarkers and exosomal biomarkers are limited. The procrastination of progress and clear results in EV research owe to the challenges including incompetent extraction methods, difficulties in characterization, and the lack of specific biomarkers.

Although exosome research has increased vigorously in the recent decade, exosome isolation techniques are still in the developing level and not standardized.[16] Exosomes are a subset of EVs which also include apoptic bodies and microvesicles. Other components in clinical blood samples such as lipoproteins, chylomicrons, and microvesicles have similar size to exosomes, making it difficult for purified isolation. The conventional EV isolation methods isolate EVs either by the physical properties (density/size) or function. UC is the gold-standard in which applies centrifugal forces to separate components according to their density.[55] However, the force used in UC changes the morphology of EVs, in top of the time consuming process with low recovery and purity. Other established methods, the size exclusion chromatography (SEC) and ultrafiltration (UC) both isolate EVs according to size differences. However, these methods also have limitations in that the pores used for isolation may be clogged resulting in low recovery and purity.[56,57] Other common disadvantages of conventional methods include expensive equipment and time consumption. This necessitates new methods and has led to development of diverse novel methods. Herein, we present a simple, practical system which isolates sEVs in a timely matter. Approximately 30 minutes are required to isolate sEVs from a single blood plasma sample. Sequential NA extraction can be managed with just additional 5 minutes. This method showed comparable purity to conventional methods (UC and TEI). Moreover, the overall process is uncomplicated, easy to repeat, and not dependent on sample volume. As this is the early validation stages for the novel sEV isolation system, there are limitations in that the extraction process must be done manually and therefore not yet suitable for large number of cases.

Despite the advantages of SF-ZAVHIS, there are several limitations to overcome for application to clinical practice. In this study, the exploration of miRNAs and circRNAs were performed in pre-selected 11 markers. However, published data on significant biomarkers, including miRNAs, circRNAs, and proteins are overflowing with universal markers such as EPCAM[58], and other markers with contradicting results needing further validation. The inconsistent results may result from technical differences, various method of data processing, and samples collected from different backgrounds.[59] For instance, even though we selected circRNAs due to the advantages including the intrinsic stability and resistance to catalysis[60,61], there was no significant results from analyzing clinical plasma samples. Validation of purely extracted sEVs from cancer cell line culture could be performed by comparing SF-ZAHVIS to UC and TEI. However, due to the limited plasma sample volume, we could not perform all three methods of sEV extraction (SF-ZAHVIS, UC, and TEI) for the clinical samples. Therefore, it is unclear whether the concentration of sEVs extracted from clinical plasma samples were adequate to detect circRNAs and identify significant difference between CRC and healthy controls. The difference in concentration and purity of sEVs, miRNAs, and circRNAs of clinical samples to cell line cultures may be the reason to the disparate results, because sEVs isolated from cell culture systems are usually obtained from large numbers of cells beyond physiologic range.[62] Moreover, utilizing circulatory exosomal miRNAs or cirRNAs for early-stage cancer diagnosis is challenging in that RNAs have low expression levels, making it even arduous combined with the task of isolating pure concentrated sEVs. The results from the present study in which there was no significant difference in miRNA expression between each stages, and of which only two miRNAs (miR-23a-3p and miR-150-5p) showed significant difference between stage 0-1 and healthy control may result from failure to overcome such difficulties.

5. Conclusion

In conclusion, the SF-ZAHVIS system is capable of isolating sEVs efficiently. By using this novel system, miRNAs could be assessed from blood plasma to distinguish CRC from healthy population. Further validation assessing clinical samples with other conventional sEV isolation techniques, in various clinical settings, with a greater number of cases collected in a prospective manner is crucial for standardizing the SF-ZAHVIS system.

6. References

1. Bray F, Ferlay J, Soerjomataram I, Siegel RL, Torre LA, Jemal A. Global cancer statistics 2018: GLOBOCAN estimates of incidence and mortality worldwide for 36 cancers in 185 countries. *CA Cancer J Clin.* 2018;68(6):394-424.
2. Petrelli F, Tomasello G, Borgonovo K, et al. Prognostic Survival Associated With Left-Sided vs Right-Sided Colon Cancer: A Systematic Review and Meta-analysis. *JAMA Oncol.* 2017;3(2):211-219.
3. Bretthauer M, Løberg M, Wieszczy P, et al. Effect of Colonoscopy Screening on Risks of Colorectal Cancer and Related Death. *N Engl J Med.* 2022;387(17):1547-1556.
4. Amri R, Bordeianou LG, Sylla P, Berger DL. Impact of screening colonoscopy on outcomes in colon cancer surgery. *JAMA Surg.* 2013;148(8):747-754.
5. Murphy CC, Sandler RS, Grubber JM, Johnson MR, Fisher DA. Underuse and Overuse of Colonoscopy for Repeat Screening and Surveillance in the Veterans Health Administration. *Clin Gastroenterol Hepatol.* 2016;14(3):436-444.e431.
6. Lin JS PL, Henrikson NB, et al. Screening for Colorectal Cancer: An Evidence Update for the U.S. Preventive Services Task Force [Internet]. Rockville (MD): Agency for Healthcare Research and Quality (US); 2021 May. (Evidence Synthesis, No. 202.) Appendix G, Adherence to Initial CRC Screening. Available from: https://www.ncbi.nlm.nih.gov/books/NBK570918/. 2021.
7. Ignatiadis M, Sledge GW, Jeffrey SS. Liquid biopsy enters the clinic - implementation issues and future challenges. *Nat Rev Clin Oncol.* 2021;18(5):297-312.
8. Tie J, Wang Y, Tomasetti C, et al. Circulating tumor DNA analysis detects minimal residual disease and predicts recurrence in patients with stage II colon cancer. *Sci Transl Med.* 2016;8(346):346ra392.
9. Vacante M, Ciuni R, Basile F, Biondi A. The Liquid Biopsy in the Management of Colorectal Cancer: An Overview. *Biomedicines.* 2020;8(9).
10. Reinert T, Schøler LV, Thomsen R, et al. Analysis of circulating tumour DNA to monitor disease burden following colorectal cancer surgery. *Gut.* 2016;65(4):625-634.
11. He F, Li L, Fan R, Wang X, Chen X, Xu Y. Extracellular Vesicles: An Emerging Regenerative Treatment for Oral Disease. *Front Cell Dev Biol.* 2021;9:669011.
12. Sheikh Hosseini M, Parhizkar Roudsari P, Gilany K, et al. Cellular Dust as a Novel Hope for Regenerative Cancer Medicine. *Adv Exp Med Biol.* 2020;1288:139-160.

13. Mashouri L, Yousefi H, Aref AR, Ahadi Am, Molaei F, Alahari SK. Exosomes: composition, biogenesis, and mechanisms in cancer metastasis and drug resistance. *Molecular Cancer.* 2019;18(1):75.
14. Nabariya DK, Pallu R, Yenuganti VR. Exosomes: The protagonists in the tale of colorectal cancer? *Biochim Biophys Acta Rev Cancer.* 2020;1874(2):188426.
15. Shang A, Gu C, Wang W, et al. Exosomal circPACRGL promotes progression of colorectal cancer via the miR-142-3p/miR-506-3p- TGF-β1 axis. *Mol Cancer.* 2020;19(1):117.
16. Sidhom K, Obi PO, Saleem A. A Review of Exosomal Isolation Methods: Is Size Exclusion Chromatography the Best Option? *Int J Mol Sci.* 2020;21(18).
17. Tang YT, Huang YY, Zheng L, et al. Comparison of isolation methods of exosomes and exosomal RNA from cell culture medium and serum. *Int J Mol Med.* 2017;40(3):834-844.
18. Zhao YJ, Song X, Niu L, Tang Y, Song X, Xie L. Circulating Exosomal miR-150-5p and miR-99b-5p as Diagnostic Biomarkers for Colorectal Cancer. *Front Oncol.* 2019;9:1129.
19. Yong FL, Wang CW, Roslani AC, Law CW. The involvement of miR-23a/APAF1 regulation axis in colorectal cancer. *Int J Mol Sci.* 2014;15(7):11713-11729.
20. Lv H, Zhang Z, Wang Y, Li C, Gong W, Wang X. MicroRNA-92a Promotes Colorectal Cancer Cell Growth and Migration by Inhibiting KLF4. *Oncol Res.* 2016;23(6):283-290.
21. Wang N, Zhu M, Tsao SW, Man K, Zhang Z, Feng Y. MiR-23a-mediated inhibition of topoisomerase 1 expression potentiates cell response to etoposide in human hepatocellular carcinoma. *Mol Cancer.* 2013;12(1):119.
22. Yang M, Tang X, Wang Z, Wu X, Tang D, Wang D. miR-125 inhibits colorectal cancer proliferation and invasion by targeting TAZ. *Biosci Rep.* 2019;39(12).
23. Liu Y, Liu R, Yang F, et al. miR-19a promotes colorectal cancer proliferation and migration by targeting TIA1. *Molecular Cancer.* 2017;16(1):53.
24. Liu T, Liu D, Guan S, Dong M. Diagnostic role of circulating MiR-21 in colorectal cancer: a update meta-analysis. *Ann Med.* 2021;53(1):87-102.
25. Li W, Chang J, Wang S, et al. miRNA-99b-5p suppresses liver metastasis of colorectal cancer by down-regulating mTOR. *Oncotarget.* 2015;6(27):24448-24462.
26. Fang F, Cheng L, Wu X, Ye M, Zhang H. miR-141 Promotes Colon Cancer Cell Proliferation by Targeted PHLPP2 Expression Inhibitionn. *Cancer Manag Res.* 2020;12:11341-11350.
27. Sameti P, Tohidast M, Amini M, Bahojb Mahdavi SZ, Najafi S, Mokhtarzadeh A. The emerging role of MicroRNA-182 in tumorigenesis; a promising therapeutic target. *Cancer Cell*

Int. 2023;23(1):134.

28. Liu L, Zhang C, Li X, et al. miR-223 promotes colon cancer by directly targeting p120 catenin. *Oncotarget.* 2017;8(38):63764-63779.
29. Morimoto M, Maishi N, Tsumita T, et al. miR-1246 in tumor extracellular vesicles promotes metastasis via increased tumor cell adhesion and endothelial cell barrier destruction. *Front Oncol.* 2023;13:973871.
30. Zheng R, Zhang K, Tan S, et al. Exosomal circLPAR1 functions in colorectal cancer diagnosis and tumorigenesis through suppressing BRD4 via METTL3-eIF3h interaction. *Mol Cancer.* 2022;21(1):49.
31. Han K, Wang FW, Cao CH, et al. CircLONP2 enhances colorectal carcinoma invasion and metastasis through modulating the maturation and exosomal dissemination of microRNA-17. *Mol Cancer.* 2020;19(1):60.
32. Ameli-Mojarad M, Ameli-Mojarad M, Hadizadeh M, et al. The effective function of circular RNA in colorectal cancer. *Cancer Cell International.* 2021;21(1):496.
33. Tie J, Cohen JD, Lahouel K, et al. Circulating Tumor DNA Analysis Guiding Adjuvant Therapy in Stage II Colon Cancer. *N Engl J Med.* 2022;386(24):2261-2272.
34. Phallen J, Sausen M, Adleff V, et al. Direct detection of early-stage cancers using circulating tumor DNA. *Sci Transl Med.* 2017;9(403).
35. Cohen JD, Li L, Wang Y, et al. Detection and localization of surgically resectable cancers with a multi-analyte blood test. *Science.* 2018;359(6378):926-930.
36. Zhang Y, Peng B, Han Y. MiR-23a regulates the proliferation and migration of human pulmonary artery smooth muscle cells (HPASMCs) through targeting BMPR2/Smad1 signaling. *Biomed Pharmacother.* 2018;103:1279-1286.
37. Peng Y, Croce CM. The role of MicroRNAs in human cancer. *Signal Transduction and Targeted Therapy.* 2016;1(1):15004.
38. Calin GA, Dumitru CD, Shimizu M, et al. Frequent deletions and down-regulation of micro-RNA genes miR15 and miR16 at 13q14 in chronic lymphocytic leukemia. *Proc Natl Acad Sci U S A.* 2002;99(24):15524-15529.
39. Schetter AJ, Okayama H, Harris CC. The role of microRNAs in colorectal cancer. *Cancer J.* 2012;18(3):244-252.
40. Luo X, Burwinkel B, Tao S, Brenner H. MicroRNA signatures: novel biomarker for colorectal cancer? *Cancer Epidemiol Biomarkers Prev.* 2011;20(7):1272-1286.

41. Ng EK, Chong WW, Jin H, et al. Differential expression of microRNAs in plasma of patients with colorectal cancer: a potential marker for colorectal cancer screening. *Gut.* 2009;58(10):1375-1381.
42. Wei QD, Zheng WB, Sun K, Xue Q, Yang CZ, Li GX. MiR-92a promotes the invasion and migration of colorectal cancer by targeting RECK. *Int J Clin Exp Pathol.* 2019;12(5):1565-1577.
43. Jahid S, Sun J, Edwards RA, et al. miR-23a promotes the transition from indolent to invasive colorectal cancer. *Cancer Discov.* 2012;2(6):540-553.
44. Jeck WR, Sharpless NE. Detecting and characterizing circular RNAs. *Nat Biotechnol.* 2014;32(5):453-461.
45. Cocquerelle C, Mascrez B, Hétuin D, Bailleul B. Mis-splicing yields circular RNA molecules. *Faseb j.* 1993;7(1):155-160.
46. Kos A, Dijkema R, Arnberg AC, van der Meide PH, Schellekens H. The hepatitis delta (delta) virus possesses a circular RNA. *Nature.* 1986;323(6088):558-560.
47. Guo JU, Agarwal V, Guo H, Bartel DP. Expanded identification and characterization of mammalian circular RNAs. *Genome Biology.* 2014;15(7):409.
48. Kristensen LS, Andersen MS, Stagsted LVW, Ebbesen KK, Hansen TB, Kjems J. The biogenesis, biology and characterization of circular RNAs. *Nature Reviews Genetics.* 2019;20(11):675-691.
49. Xie Y, Li J, Li P, et al. RNA-Seq Profiling of Serum Exosomal Circular RNAs Reveals Circ-PNN as a Potential Biomarker for Human Colorectal Cancer. *Front Oncol.* 2020;10:982.
50. Brennan K, Martin K, FitzGerald SP, et al. A comparison of methods for the isolation and separation of extracellular vesicles from protein and lipid particles in human serum. *Scientific Reports.* 2020;10(1):1039.
51. Langevin SM, Kuhnell D, Biesiada J, et al. Comparability of the small RNA secretome across human biofluids concomitantly collected from healthy adults. *PLoS One.* 2020;15(4):e0229976.
52. Lin J, Li J, Huang B, et al. Exosomes: novel biomarkers for clinical diagnosis. *ScientificWorldJournal.* 2015;2015:657086.
53. Brinton LT, Sloane HS, Kester M, Kelly KA. Formation and role of exosomes in cancer. *Cell Mol Life Sci.* 2015;72(4):659-671.
54. Dohmen J, Semaan A, Kobilay M, et al. Diagnostic Potential of Exosomal microRNAs in Colorectal Cancer. *Diagnostics (Basel).* 2022;12(6).

55. Théry C, Amigorena S, Raposo G, Clayton A. Isolation and characterization of exosomes from cell culture supernatants and biological fluids. *Curr Protoc Cell Biol.* 2006;Chapter 3:Unit 3.22.

56. Cheruvanky A, Zhou H, Pisitkun T, et al. Rapid isolation of urinary exosomal biomarkers using a nanomembrane ultrafiltration concentrator. *Am J Physiol Renal Physiol.* 2007;292(5):F1657-1661.

57. Baranyai T, Herczeg K, Onódi Z, et al. Isolation of Exosomes from Blood Plasma: Qualitative and Quantitative Comparison of Ultracentrifugation and Size Exclusion Chromatography Methods. *PLoS One.* 2015;10(12):e0145686.

58. Gires O, Pan M, Schinke H, Canis M, Baeuerle PA. Expression and function of epithelial cell adhesion molecule EpCAM: where are we after 40 years? *Cancer and Metastasis Reviews.* 2020;39(3):969-987.

59. Chen X, Shi K, Wang Y, et al. Clinical value of integrated-signature miRNAs in colorectal cancer: miRNA expression profiling analysis and experimental validation. *Oncotarget.* 2015;6(35):37544-37556.

60. Pisignano G, Michael DC, Visal TH, Pirlog R, Ladomery M, Calin GA. Going circular: history, present, and future of circRNAs in cancer. *Oncogene.* 2023;42(38):2783-2800.

61. Zhang XO, Dong R, Zhang Y, et al. Diverse alternative back-splicing and alternative splicing landscape of circular RNAs. *Genome Res.* 2016;26(9):1277-1287.

62. Kalluri R, LeBleu VS. The biology, function, and biomedical applications of exosomes. *Science.* 2020;367(6478).

국 문 요 약

목적: 대장암의 조기 발견은 효과적인 개입을 위해 중요하며, 5년 생존율이 병기가 높음에 따라 급격히 저하되기 때문에 중요하다. 대장 내시경을 통한 감시가 표준 진단 방법이지만 침습성 및 접근성 문제와 같은 제한이 있다. 최근 대장암 진단에서 작은 세포외 소포체(sEVs)를 포함한 액체 생검이 중요성을 얻고 있다. 본 연구의 목적은 새로운 EV 분리 시스템을 적용하여 대장암 환자와 건강인의 RNA 발현을 비교하는 것이다.

대상 및 방법: 서울의 아산의료원 생물자원센터(BRC)에서 80명의 대장암 환자와 20명의 건강한 대조군의 혈장 샘플을 얻었다. 대상군은 병리학적으로 확인된 0 ~ 1기 (n = 20), 2기 (n = 20), 3기 (n = 20) 및 4기 대장암 환자 (n = 20) 및 건강한 대조군 (n = 20)으로 구성되었다.

EV 분리, EV 유래 핵산(NA) 추출을 위한 시스템(SF-ZAHVIS)을 사용하여 혈장 샘플로부터 EV를 분리했다. EV 유래 miRNA 및 circRNA는 실시간 폴리머아제 연쇄반응(qRT-PCR)을 사용하여 추출되었으며, 건강한 대조군 및 각 암 병기에 따라 비교되었다. EV 분리 시스템의 효과는 전통적인 엑소좀 분리 기술 (초고속 원심분리법 [UC] 및 Total exosome isolation [TEI] 방법)과 비교를 통해 평가했다.

결과: SF-ZAHVIS는 효율적인 EV 분리를 보여주었으며, UC 및 TEI 기술과 유사한 순도와 농도를 얻었다. 신호 강도와 수에 기반한 EV의 입자 크기 분포는 나노입자 추적 분석을 통해 결정되었으며, SF-ZAHVIS는 187.1 ± 27.5, UC는 202.4 ± 36.7, TEI는 222.5 ± 65.3 nm로 나타났다. SF-ZAHVIS 시스템은 대장암 miRNA 마커인 miR-23a-3p, miR-92a-3p, miR-125a-3p, miR-150-5p를 성공적으로 검출했다. miR-23a-3p, miR-92a-3p 및 miR-125a-3p의 상대 발현 수준은 대조군과 비교하여 유의적으로 높았으며 (P = 0.014, 0.0002 및 0.0274), miR-150-5p의 발현 수준은 대장암 군에서 대조군에 비해 유의하게 낮았다 (P < 0.0001).

결론: SF-ZAHVIS 시스템은 EV를 효율적으로 분리할 수 있으며, 이 시스템을 사용하여 혈장에서 miRNA를 평가하여 대장암을 진단할 수 있다.